Spectral Coherence Model for Power Fluctuations in a Wind Farm

A. Vigueras-Rodríguez [a,*], P. Sørensen [b], A. Viedma [a]

[a] *Thermal and Fluids Egineering Department, Universidad Politécnica de Cartagena. Cartagena, Murcia, Spain.*

[b] *Wind Energy Department, Risø National Laboratory, Roskilde, Denmark*

Abstract

This paper attends to the modelling of power fluctuations of large offshore wind farms, concretely this paper focuses in the analysis of the spectral coherence models for the wind speed.

So, firstly the current coherence models are analysed from the point of view of the Power Fluctuation. Then the paper shows the need of a new coherence model adapted to this frame i.e. to the characteristic length and height of nowadays wind farms and the characteristic time of the power fluctuation.

This paper provides an adapted coherence model. That model has been developed using wind speed and power measurements from the 72 Wind Turbines and 2 of the meteorological masts from Nysted Offshore Wind Farm during 9 months.

Key words: wind models, wind coherence, power fluctuation, offshore wind farms
PACS: 89.30.Ee

1 Introduction

Nowadays the concern about the effects of the pollution (like the global warming effect) and the knowledge of the limitations of the fossil resources are creating a strong tendency in Europe towards the use of renewable energy sources. Therefore, there has been a big growth in the Wind Energy development, and it is expected to go on rising. Such growths make essential to research deeply into this energy technology from the point of view of an important component

* Corresponding author.
Email address: avigueras.rodriguez@upct.es (A. Vigueras-Rodríguez).

of the electrical system, instead of considering it a very small part of it as it was done previously.

A major issue in the control and stability of electric power systems is to maintain the balance between generated and consumed power. Because of the fluctuating nature of wind speeds, the increasing use of wind turbines for power generation has risen the interest in the fluctuations of the wind turbines power production, especially when the wind turbines are concentrated geographically in large wind farms. That fluctuation can also be a security issue in the future for systems with weak interconnections like Ireland or the Iberian Peninsula.

As example of the significance of these power fluctuations in Energinet.dk (the Danish Transmission System Operator), according to [1], Energinet.dk has observed that power fluctuations from the 160 MW offshore wind farm Horns Rev in West Denmark introduce several challenges to reliable operation of the power system in West Denmark. And also, that it contributes to deviations from the planned power exchange with the Central European Power System (UCTE). Moreover, it was observed that the time scale of the power fluctuations was from tens of minutes to several hours.

And in those fluctuations the importance of the spatial correlation of the wind speed in that time frame is shown by the fact that the power fluctuations of the 160 MW Wind Farm was significantly greater than the fluctuations in 160 MW of WTs distributed in smaller onshore Wind Farms.

The conclusions make the research of the spatial correlation a main topic for the power fluctuation analysis.

2 Coherence models for Power Fluctuation

The spectral coherence between the wind speed in two different points is defined by

$$\gamma(f) = \frac{S_{ab}(f)}{\sqrt{S_{aa}(f)S_{bb}(f)}} \tag{1}$$

where $S_{ab}(f)$ is the crossed power spectral density (CPSD) between the wind speed in points a and b, and $S_{aa}(f)$ and $S_{bb}(f)$ are the power spectral density (PSD) of the wind in each point.

Those spectral functions are given by the following equation:

$$S_{ab}(f) = \left[\mathbf{F}\left(\phi_{u,ab}(\tau)\right)_{(f)}\right] \tag{2}$$

being $\mathbf{F}$ the Fourier Transform and $\phi_{u,ab}(\tau)$ the cross correlation of the wind speed between the points a and b, defined by $\phi_{u,ab}(\tau) = \frac{1}{T}\int_T V_a(t)V_b(t-\tau)dt = \frac{1}{T}u_a(t) * u_b(-t)$, where "$*$" is the convolution operator.

Besides the practical observation of the link between the power fluctuation and the spectral coherence above cited, different theoretical and practical observations appeared in recent papers like [4] and [7] confirm that the seeking of power fluctuations models is totally linked with the coherence models in a WF frame.

Regarding the current coherence models, most of them are based in modifications to the Davenport model [2]. Davenport's model suggest an exponential behaviour explained by the following expression

$$|\gamma| = e^{-a\frac{d\cdot f}{V}} \tag{3}$$

where a, that is usually called decay factor, is a constant.

This model does not explain the inflow angle dependence, and so the usual modifications of this model, based in changing the value of the constant a or even in suggesting a stochastic behaviour for it [6], have the same problem when using them in the scale of a wind farm, where this dependence is essential [9].

Nevertheless, the modifications suggested by Schlez & Infield [5] introduces that dependency expressing a as a function of the inflow angle

$$a = \sqrt{(a_{long}\cdot\cos\alpha)^2 + (a_{lat}\cdot\sin\alpha)^2} \tag{4}$$

being a_{long} and a_{lat} respectively the decay factors for the longitudinal and the lateral situations given by

$$a_{long} = (15 \pm 5)\cdot I_V \tag{5}$$

$$a_{lat} = (17.5 \pm 5)(m/s)^{-1}\cdot I_V \cdot \bar{V} \tag{6}$$

being I_V the turbulent intensity defined by $I_V = \frac{\sigma_v}{\bar{V}}$

However, this empirical model was based on a very limited distance scale and so it does not predict the behaviour in the large wind farms of nowadays [9], so none of the usual models used in Wind Energy suits for studying the Power Fluctuation of Wind Farms. Therefore, in this paper the spectral coherence within a large wind farm is studied, with the aim of suggesting a suitable model.

3 Experimental data used

The data used in this work is based in the Nysted Wind Farm, which is an offshore Wind Farm compound of 72 Siemens SWT-2.3-82 fixed speed wind turbines, with a global nominal power of 165.6 MW and distances between the wind turbines between 0.48 km and 7.73 km.

In the 72 WTs and the 2 Meteorological Masts shown in the figures, it has been measured the wind speed in the nacelle of each WT (69 m above ground), the active power produced, the yaw angle, the angular velocity and other variables. Furthermore, we have accesed to the wind speed and wind direction data from the meteorological masts at 70 m. above ground.

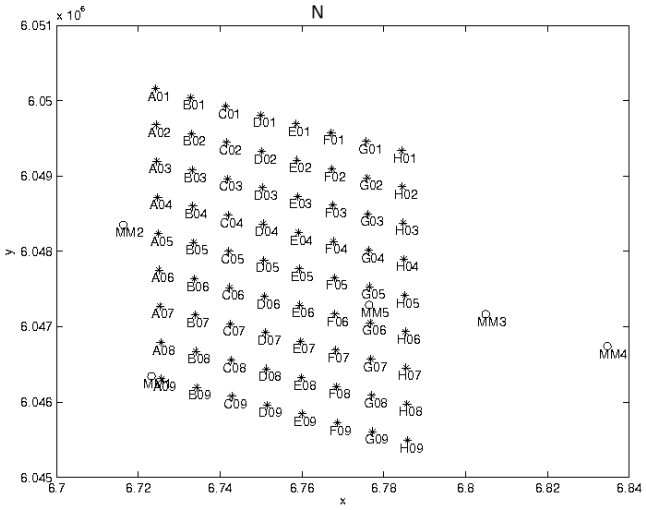

Figure 1. Layout of the Nysted Wind Farm

All of those data have been obtained through a SCADA system used by the wind farm main controller, which logs the data with a 1Hz sampling frequency.

The data stored that have been used for this work is basically the wind speeds measured by each WT and the velocity and direction of the wind measured in the masts MM2 and MM3 that are shown in the figure 1, corresponding to 9 months in 2005.

4 Procedure of the coherence measuring

For obtaining a coherence model in a suitable time frame for this purpose, 2 hour intervals have been considered. Next, it has been selected only intervals with a 75% of valid data in MM_2 and MM_3. For the single Wind Turbine data a filtering for each Wind Turbine working in a "normal" state has been

done by selecting the WTs with at least a 90% of valid data and holes smaller than 3 seconds, so that they can be fulfilled using splines without having any significant influence to the time scale that we are studying.

Then, it has been define similar pairs of WTs with similar distances and angles like A_{01}-A_{02} and C_{03}-C_{04}, calling them segments.

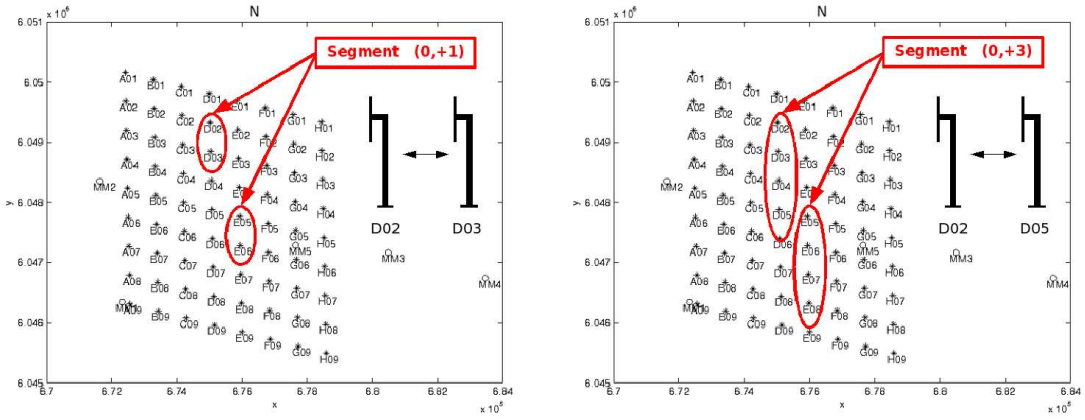

Figure 2. Example of how the segments are assembled

Following this process, as it is shown in figure 2, we consider all segments with more than 8 couples, as example some of those segments are shown in the table 1.

Δi_{row}	Δi_{column}	d_{xy}(m)	β_{xy}(deg.)	Blocks
0	1	482	92	64
0	2	964	92	56
0	3	1445	92	48
1	1	1062	146	56
5	4	5041	150	15
1	-4	1972	67	35

Table 1
Example of the 2-point segment characteristics

Once having selected the intervals, the data in each time interval are processed, averaging the power spectra of each couple of WTs belonging to the same segment.

For instance, when we consider the segment n compound of m pairs (being $m \geq 8$) of WTs with valid data (a_i, b_i), regarding equation 2 and the convolution property of the Fourier Transform:

$$S_{aa} = \frac{\sum_{i=1}^{m} \mathbf{FFT}(V_{a_i}) \cdot \mathbf{FFT}(V_{a_i})^*}{m} \tag{7}$$

$$S_{bb} = \frac{\sum_{i=1}^{m} \mathbf{FFT}(V_{b_i}) \cdot \mathbf{FFT}(V_{b_i})^*}{m} \tag{8}$$

$$S_{ab} = \frac{\sum_{i=1}^{m} \mathbf{FFT}(V_{a_i}) \cdot \mathbf{FFT}(V_{b_i}^*)}{m} \tag{9}$$

where $S_{aa}(f), S_{bb}(f) \in \mathbb{R}$, as well as $S_{ab}(f) \in \mathbb{C}$. This is done for each segment with enough valid data in each time interval.

Afterwards, the results of each segment data $(S_{aa}(f), S_{bb}, (f)S_{ab}(f))$ can be classified depending on the average wind speed $\overline{V}$ and the inflow angle α calculated through the segment angle β and the wind direction ϕ.

Next, the data classified for each segment (n) in the same wind speed range (v_m) and inflow angle range (α_k) are used for calculating the coherence $\gamma(n, v_m, \alpha_k, f)$ as follows:

$$\gamma(n, v_m, \alpha_k, f) = \frac{\sum_{i=1}^{N_n} S_{ab}(i, f) \cdot N_i}{\sqrt{\sum_{i=1}^{N_n} S_{aa}(i, f) \cdot N_i \cdot \sum_{i=1}^{N_n} S_{aa}(i, f) \cdot N_i}} \tag{10}$$

where N_i are the number of pairs of WT series of data used previously for calculating the power spectral functions, i.e. the number m in equations 7,8 and 9.

The followind 5 inflow angle bins are used $[0, 6, 25, 65, 84, 90]$(deg.), whereas the ranges of wind speed are $2m/s$ intervals from $2m/s$ to $16m/s$.

Finally, using the distance of each segment $d(n)$, we get an experimental $\gamma(d, v_m, \alpha_k, f)$.

In this proceeding the wake has been neglected, that is possible because in most of the pairs consider where both measures are inside of the overall wake, that effect affects similarly to both series of data and so, it is removed by the definition of the coherence itself (eq. 1). On the other hand, in the cases where the influence of having measures out of the wake and measures in the deep wake could be greater, looking at the expression of power spectral density of the wind inside and out of the wake that is shown in [7], we see that it does not affect to the time scale which we are interested in.

In the data considered the average of the turbulent intensity is $\overline{I_V} = 0.12$, the turbulent intensity has not been introduced into the general analysis in order to simplify the problem, so that enough number of long distance series are available. However, afterwards the influence of I_V is analysed meanwhile using

the following I_V ranges: $[0.04, 0.10]$ with an average $\overline{I_V} = 0.09$, $[0.08, 0.16]$ with $\overline{I_V} = 0.12$ and finally $[0.12, 0.20]$ with $\overline{I_V} = 0.15$.

5 Results

As it has been explained previously we have a package of coherence data ($|\gamma(d, v_m, \alpha_k, f)|$ and its argument $\angle\gamma(d, v_m, \alpha_k, f)$), from which we focus mainly in the module part.

Looking to the data corresponding to the longitudinal situation ($\alpha_1 \Rightarrow \alpha \in [0,\, 6\,\text{deg}]$) plotted in figure 3, where the decay factor a (see 3) is plotted for different wind speed ranges against the distance, it is possible to see that there is not any significant tendency in the variation of that parameter with the distance or the wind speed ($a_{long} \neq f(d, V)$). Therefore, it is possible to assume that a constant value for the longitudinal situation a_{long} (see 5) would be suitable in this distance and time frame. This would agree qualitatively (but not quantitatively) to Schlez & Infield model (Eq. 4).

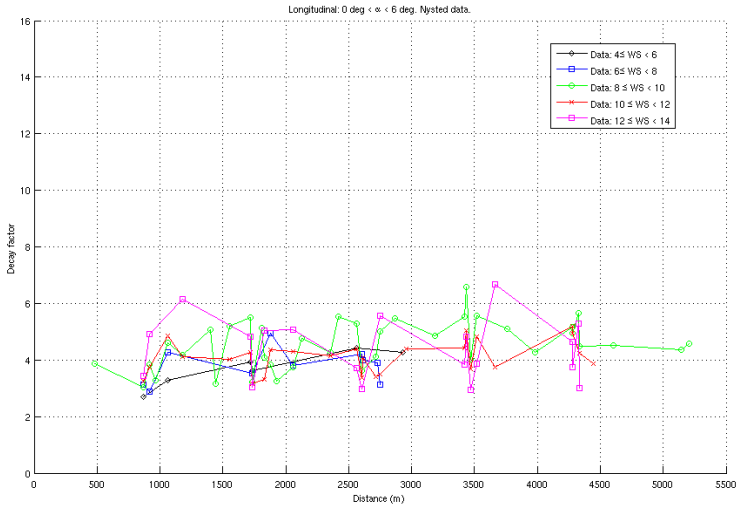

Figure 3. Decay factor of the coherence in the longitudinal situation.

However, the lateral decay factor parameter depends significantly on the distance and the wind speed ($a_{lat} = f(d, V)$), as it is shown in figure 4, and this was not predict by the Schlez & Infield model due to the different time and length scale in the distance between the points (100 m) and in the height above ground (18 m).

Looking into the figure, it is possible to see that in this case, a_{lat} gets lower when the distance rises, a_{lat} rises when wind speed gets greater, and those changes of a_{lat} get smaller as the distance gets greater.

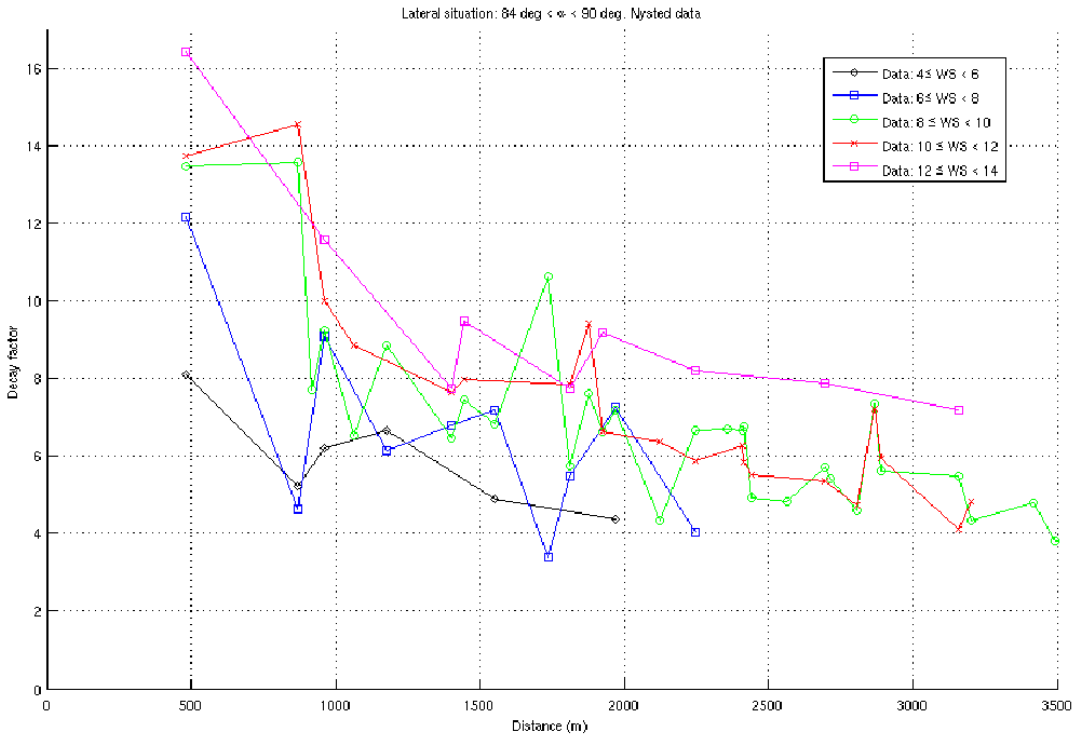

Figure 4. Decay factor of the coherence in the lateral situation.

Looking at the intermediate situations, like the one shown in figure 5, it is possible to see an intermediate behaviour between the longitudinal and the lateral situation, thus working with a model based on the Schlez & Infield one seems convenient.

6 Fitting of the model

Firstly, some models were suggest after looking the figures shown previously in section 5. Those models consisted in a decay factor build through the equation 4, considering a_{long} as constant, whereas a_{lat} was consider a function that complies with the following conditions:

$$d \uparrow \Rightarrow a_{lat} \downarrow \tag{11}$$
$$V \uparrow \Rightarrow a_{lat} \uparrow \tag{12}$$
$$d \uparrow\uparrow \Rightarrow \Delta a_{lat}(\Delta d, \Delta V) \downarrow \tag{13}$$

Next, the decay factors a_{long} and the parameters from the function a_{lat}, were fitted using only the data from the longitudinal and the lateral situation respectively (α_1 and α_5), this was done by minimising the error of the model

when trying to estimate $\log(\gamma)$, reducing it to a linear optimisation process, in which each segment data is weighted by $N_{S_n} = \sum_i^{N_n} N_i$ (see equation 10).

Afterwards, using those values as initial point of a simplex method the model is fitted to the overall data $|\gamma(d, V, \alpha, f)|$. Arriving to the following model:

$$|\gamma(d, V, \alpha, f)| = e^{\sqrt{(a_{long}\cdot\cos\alpha)^2+(a_{lat}(d,V)\cdot\sin\alpha)^2}\frac{d\cdot f}{V}} \tag{14}$$

$$a_{long} \approx 4.5 \tag{15}$$

$$a_{lat}(d, V) \approx 466(s)\frac{V}{d} + 4.2 \tag{16}$$

This model fits quite well to the original data, having a standard deviation for the coherence data previously calculated $|\gamma(d(n), V, \alpha, f)|$ in each segment n smaller than 0.06, i.e.:

$$\sigma_\gamma = \sqrt{\frac{\sum_n N_{S_n} \cdot \left(|\gamma(d(n), V, \alpha, f)| - |\hat{\gamma}(d, V, \alpha, f)|\right)^2}{\sum_n N_{S_n}}} < 0.06 \tag{17}$$

A comparison with the original coherence data in four different situations can be found in figure 9. Regarding the decay factors, some comparisons for different wind speeds, distances and inflow angles are provided in figures 6, 7

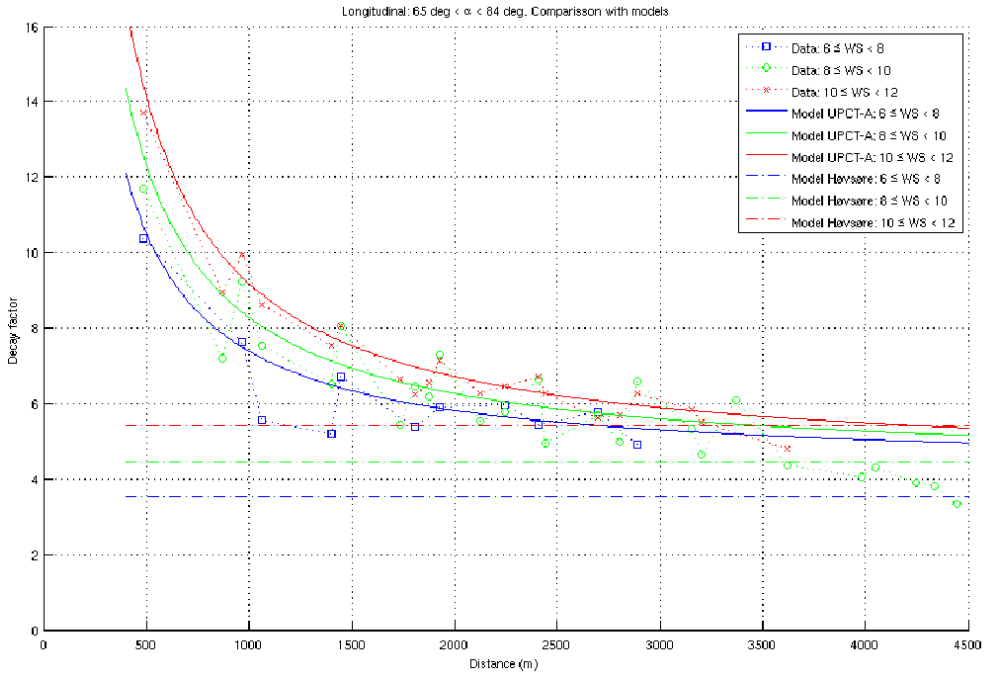

Figure 5. Decay factor of the coherence for inflow angles between 65 deg. and 84 deg.

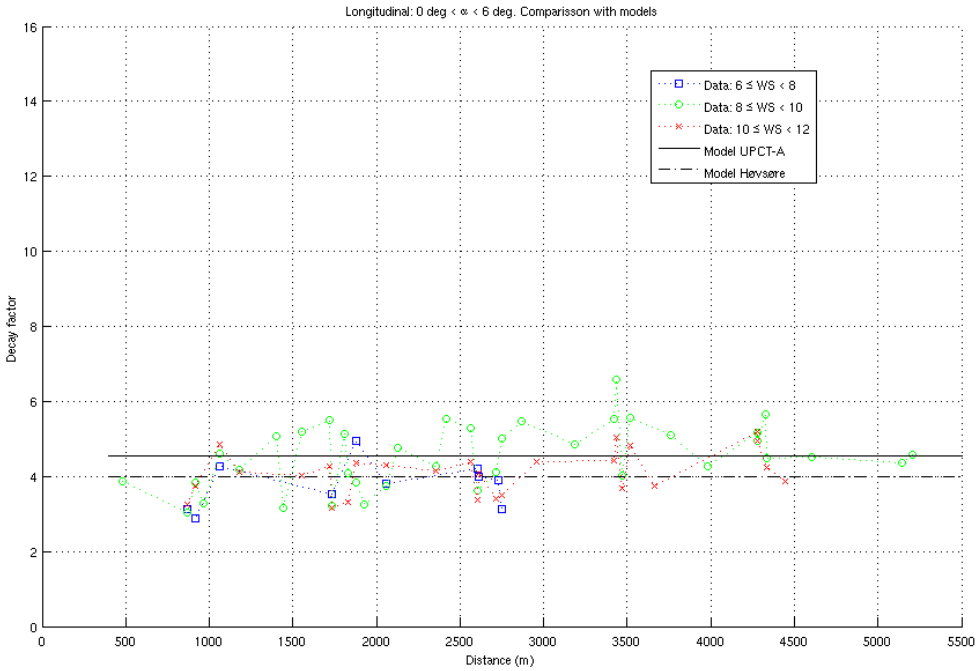

Figure 6. Comparison between the "measured" decay factors and the model in the longitudinal situation.

and 8, showing all of them a good agreement between the experimental data and the model.

As it was expected that model tends to behave similarly to the one proposed by Schlez & Infield when a small (and constant) distance is chosen (a_{long} =cte. and $a_{lat} \sim V$) but in this case the dependence with the distance has been introduced.

Note: ¿¿Should I write something about the coherence angle?? ...

Furthermore, as the constant values of the model (Eq. 14) are very closed, it is possible to simplify the model considering them equal without increasing significantly the error, so in this way we can express the coherence as follows

$$|\gamma(d, V, \alpha, f)| = e^{\sqrt{(a_{long}\cdot\cos\alpha)^2+(a_{lat}(d,V)\cdot\sin\alpha)^2}\frac{d\cdot f}{V}} \tag{18}$$

$$a_{long} \approx 4.4 \tag{19}$$

$$a_{lat}(d, V) \approx 436(s)\frac{V}{d} + a_{long} \tag{20}$$

Regarding the influence of the I_V, neglected in the general proceeding as explained in section 4, in the equation 14 it does not have a considerable influence in the longitudinal term, meanwhile when I_V rises the non-dimensional term rises and the other term gets reduced proportionally to the square root of that

increase. So, the influence I_V could be introduced in this way:

$$|\gamma(d, V, \alpha, f)| = e^{\sqrt{(a_{long}\cdot\cos\alpha)^2+(a_{lat}(d,V)\cdot\sin\alpha)^2}\frac{d\cdot f}{V}} \tag{21}$$

$$a_{long} \approx 4.5 \tag{22}$$

$$a_{lat}(d, V) \approx \frac{56(s)}{\sqrt{I_V}} \cdot \frac{V}{d} + 35 \cdot \sqrt{I_V} \tag{23}$$

Nevertheless, its influence is not that significant and it can be neglected increasing the simplicity and not affecting to the reliability of the model. Moreover, in the simplified model (eq. 18), the influence of I_V in the lateral "time constant" is quite small.

7 Conclusions

Starting from 9 months of real data coming from a Large Offshore Wind Farm, it has been seen that there is a significant dependence between the coherence and the inflow angle, as in the model suggested by Schlez & Infield. However, it was also shown that in the length, height and time scale interesting for studying the power fluctuations of Large Wind Farms, there is a strong

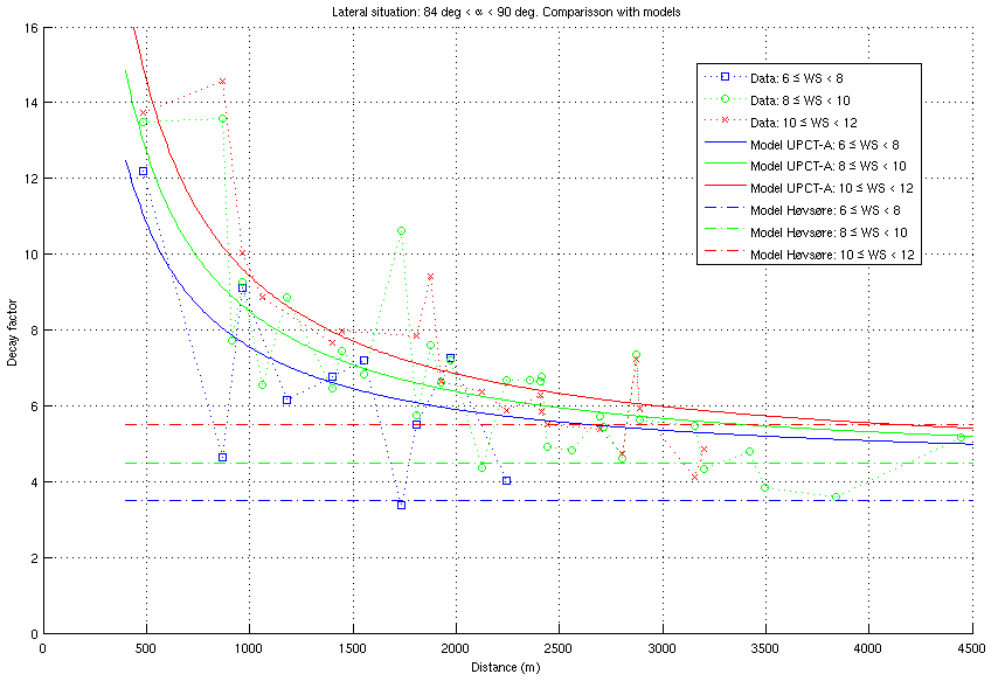

Figure 7. Comparison between the "measured" decay factors and the model in the lateral situation.

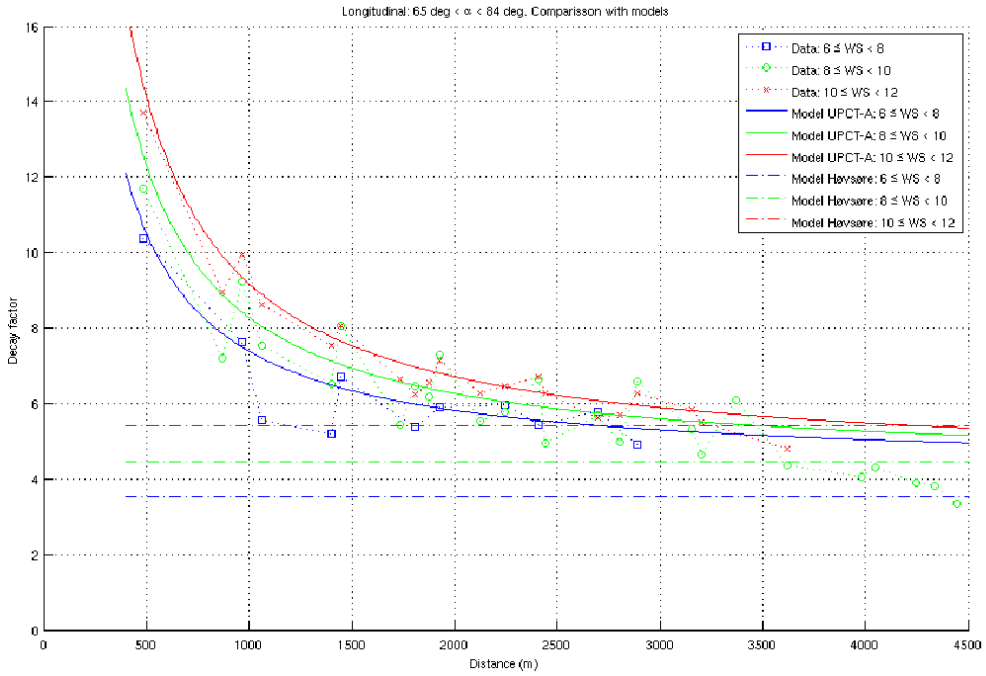

Figure 8. Comparison between the "measured" decay factors and the model for inflow angles between 65 deg. and 84 deg.

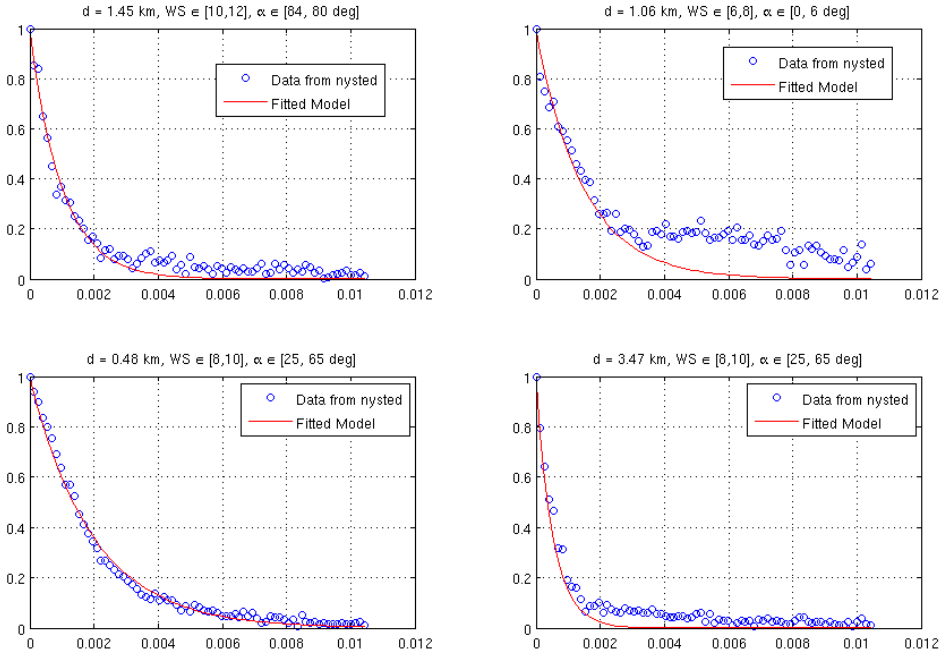

Figure 9. Comparison between the "measured" coherence and the fitted model in 4 different situations

dependency between the decay factor in the lateral situation and the distance and wind velocity.

From those differences, a model for the spectral coherence of the wind velocity has been developed.

That empirical model has been fitted in a time scale up to 2 hours and with distances from near 500 m to 6 km. The election of the scale, based in the bibliography above cited, makes this model suitable in the frame of Power Fluctuation.

This coherence model and its simplification have been added to the PARK-SIMU program, that is being introduce as a plug-in for the commercial program DIgSILENT, so that it will be possible to use it for power fluctuation studies in offshore wind farms, and even for evaluating the shape of big wind farms from this point of view.

Wake and other effects can be introduced for instance as it is described in [3, 7, 8].

8 Acknowledgements

The work presented in this paper has been done in the research project "Power Fluctuations from large offshore wind farms" financed by the Danish Transmission System Operator Energinet.dk as PSO 2004 project number 6506.

A. Vigueras-Rodríguez is supported by the Spanish Ministerio de Educación y Ciencia through the grant program "Becas FPU".

References

[1] V. Akhmatov, J. P. Kjaergaard, and H. Abildgaard. Announcement of the large offshore wind farm horns rev b and experience from prior projects in denmark. In *European Wind Energy Conference, EWEC 2004*, 2004.

[2] A. G. Davenport. The spectrum of horizontal gustiness near the ground in high winds. *Quarterly Journal of Meteorology Society*, 87(372):194–211, 1961.

[3] S. Frandsen. Turbulence and turbulence-generated structural loading in wind turbine clusters. Technical report, Risø National Laboratory, 2005.

[4] T. Nanahara, M. Asari, T. Sato, K. Yamaguchi, M. Shibata, and T. Maejima. Smoothing effects of distributed wind turbines. part 1. coherence and smoothing effects at a wind farm. *Wind Energy*, 7:61–74, 2004.

[5] W. Schlez and D. Infield. Horizontal, two point coherence for separations greater than the measurement height. *Boundary-Layer Meteorology*, 87:459–480, 1998.

[6] G. Solari. Turbulence modeling for gust loading. *ASCE Journal of Structural Engineering*, 113(7), 1987.

[7] P. Sørensen, N. Cutululis, A. Vigueras-Rodríguez, H. Madsen, P. Pinson, L. Jensen, J. Hjerrild, and M. Donovan. Modelling of power fluctuations from large offshore wind farms. Wind Energy.

[8] P. Sørensen, A. D. Hansen, and P.E. Carvalho Rosas. Wind models for simulation of power fluctuations from wind farms. *Journal of Wind Engineering and Industrial Aerodynamics*, 90:1381–1402, 2002.

[9] A. Vigueras-Rodríguez, P. Sørensen, and A. Viedma. Spectral coherence models for the wind speed in large wind farms. In *Proceedings of the 2nd PhD Seminar on Wind Energy in Europe*, Roskilde (Denmark), 2006. European Academy of Wind Energy.